Geodesy and Geodynamics 13 (2022) 160–169

Contents lists available at ScienceDirect

Geodesy and Geodynamics

journal homepage: http://www.keaipublishing.com/geog

A review of methods for mitigating ionospheric artifacts in differential SAR interferometry

Bochen Zhang [a, b], Wu Zhu [c, *], Xiaoli Ding [d], Chisheng Wang [a, e], Songbo Wu [d], Qin Zhang [c]

[a] MNR Key Laboratory for Geo-Environmental Monitoring of Great Bay Area & Guangdong Key Laboratory of Urban Informatics & Shenzhen Key Laboratory of Spatial Smart Sensing and Services, Shenzhen University, 518060 Shenzhen, China
[b] College of Civil and Transportation Engineering, Shenzhen University, 518060 Shenzhen, China
[c] School of Geology Engineering and Geomatics, Chang'an University, Xi'an, Shaanxi, China
[d] Department of Land Surveying and Geo-Informatics, The Hong Kong Polytechnic University, Kowloon, Hong Kong, China
[e] School of Architecture & Urban Planning, Shenzhen University, 518060 Shenzhen, China

ARTICLE INFO

Article history:
Received 25 September 2021
Received in revised form
2 December 2021
Accepted 7 December 2021
Available online 30 December 2021

Keywords:
InSAR
Ionospheric artifacts
Azimuth pixel shift
Faraday rotation
Range split-spectrum

ABSTRACT

Interferometric synthetic aperture radar (InSAR) has been widely used to measure ground displacements related to geophysical and anthropic activities over the past three decades. Satellite SAR systems use microwave signals that interact with the ionosphere when they travel through it during the imaging processes. In this context, ionospheric variations can significantly contaminate SAR imagery, which in turn affects spaceborne InSAR measurements. This bias also leads to a decrease in the coherence and accuracy of InSAR measurements, especially for the low-frequency SAR systems. In this paper, we give an overview of the latest methods for mitigating the ionospheric contributions in InSAR, including Faraday rotation method, azimuth shift method, and range split-spectrum method, and only focus on the single pair of InSAR interferograms. The current challenges and future perspectives are outlined at the end of this paper.

1. Introduction

As a widely used technique, spaceborne interferometric synthetic aperture radar (InSAR) is an effective method for measuring the crustal deformation or digital elevation model (DEM) of the Earth's surface [1–3]. This technique is advantageous in remotely monitoring the Earth's surface with wide geographic coverage, weather-independent capacity, and high measurement accuracy. And it has been broadly used in many applications related to geophysical and anthropic activities, such as seismic deformation [4,5], glacier motions [6,7], volcanic eruptions [8,9], underground mining [3,10], groundwater extracting [11], land reclamation [12], and infrastructures instabilities [3,13–16].

Satellite SAR systems are generally at an altitude of 500 km above the Earth's surface. Therefore, the transmitted and received signals interact with two main layers of the atmosphere (troposphere and ionosphere) as they pass through the atmosphere. If the refractive index varies in the troposphere and ionosphere, the data artifacts will be introduced in the focused SAR images, and the accuracy of InSAR measurement can be accordingly degraded [17–20]. The ionospheric variations cause data artifacts on InSAR observations with different scales, which is mainly dependent on the data acquisition time (daytime or night-time), the wavelength of SAR data, changes of the ionospheric total electron content (TEC), the geographic location of the study area (low, middle, and high latitudes), and factors induced by the events from external and internal of the Earth (i.e., solar magnetic storm, geomagnetic abnormity, and mega earthquake) [21–24].

Developing methods for correcting the ionospheric artifacts is an essential topic for applications of InSAR. There are two main aspects of mitigating the ionospheric artifacts on InSAR, i.e., to improve the accuracy of InSAR measurements and reveal the “true”

* Corresponding author.
E-mail address: zhuwu@chd.edu.cn (W. Zhu).
Peer review under responsibility of Institute of Seismology, China Earthquake Administration.

Production and Hosting by Elsevier on behalf of KeAi

https://doi.org/10.1016/j.geog.2021.12.001

features of monitoring scenarios. Several studies have been carried out in recent years to mitigate the ionospheric artifacts in InSAR. This paper provides an overview of the latest developments in mitigating the ionospheric artifacts in InSAR, focusing only on single pair of the differential InSAR.

2. InSAR and ionosphere

2.1. InSAR

As a coherent active microwave imaging technique, SAR provides a unique illumination by recording the scattering properties of the Earth's surface under almost all-weather conditions during day and night [25]. SAR systems based on airborne or spaceborne platforms obey the same fundamental principle, as sketched in Fig. 1. The raw images are collected by transmitting microwave signals from an antenna along the satellite flight direction; then the returned echoes during a period of backscattering are recorded by the received antenna; after the returned pulses are collected, the images are focused using the SAR imaging algorithm, such as Range-Doppler and Chirp Scaling processing [26].

By measuring the phase differences between two SAR images, the ground deformation at different times over the same region is obtained using the InSAR technique. The shifts of the returned phase induced by geophysical and anthropic activities are precisely measured. The phase shifts between two SAR acquisitions are proportional to the difference of slant range distance. Then, the complex image from one acquisition is multiplied with the complex conjugate data from another acquisition to generate the interferogram. In the case with a non-zero baseline, the differential interferometric phase is a combination of phase components, including those from the flat term $\Delta\phi_{\text{flat}}$, topographic phase term $\Delta\phi_{\text{topo}}$, ground deformation phase term $\Delta\phi_{\text{def}}$, and atmospheric phase terms, i.e., tropospheric $\Delta\phi_{\text{trop}}$ and ionospheric $\Delta\phi_{\text{ion}}$ contributions, which can be expressed as: $\Delta\phi_{\text{InSAR}} = \Delta\phi_{\text{flat}} + \Delta\phi_{\text{topo}} + \Delta\phi_{\text{trop}} + \Delta\phi_{\text{ion}} + \Delta\phi_{\text{def}}$. After subtraction or elimination of other phase terms, the deformation in the light of sight (LOS) direction is extracted. However, some phase contributions, such as tropospheric, residual topographic, and orbital errors, are sometimes difficult to remove on an individual InSAR interferogram, and many studies have been conducted to mitigate them on multitemporal InSAR [18,27–31]. In addition to the phase errors compensation, the modern technique of distributed scatterer can improve the quality of the interferometric phase by increasing the signal-to-noise ratio (SNR) [32–34].

The above is a brief introduction to the conventional differential InSAR (D-InSAR) method, and more details can be found in some review articles [25,26,35,36].

2.2. Ionosphere

As a portion of the upper atmosphere, the ionosphere surrounds the Earth and extends from about 60 km to beyond 1000 km. It is mainly comprised of free electrons, ions, and neutral particles. Under the action of extreme ultraviolet radiation from the Sun, a mixture of free electrons, ions, and neutral gases is produced by the neutral particles in the ionosphere. Besides the solar ultraviolet, there are other sources for ionization in the ionosphere, such as soft X-ray radiation, cosmic rays, and collisions with energetic particles at high latitudes [22].

The ionosphere is a highly dynamic and anisotropic medium. It varies in both space and time domain on a daily basis, which is closely correlated to the activities of the Sun. The density of electrons in the ionosphere changes dramatically from the local daytime to night-time, reaching the maximum in the early afternoon and gradually decreasing after midnight, as shown in Fig. 2. Thus, the ionospheric activity is more stable during the day than at night. For this reason, the ascending SAR images are more easily affected by the ionospheric variations than the descending images [24].

According to the different physical and chemical properties at different altitude levels, the ionosphere structure can be generally divided into four different layers (D, E, F1, and F2), especially the electron density profile presents a layered structure [22]. Moreover, the ionospheric electron density and the main source of ionization in these layers are different.

2.3. Effect of the ionosphere on SAR and InSAR

A detailed summary of the ionospheric effects on satellite SAR images has been conducted by Xu et al. [23]. The effects of the ionosphere are mainly contributed by the background ionosphere and ionospheric irregularities, including dispersion, group delay, phase advance, Faraday rotation (FR), pixel shift, image degradations, and defocusing [19,23,37,38]. The effect of FR is different for each polarization plan, i.e., HH, HV, VH, and VV, and the absolute

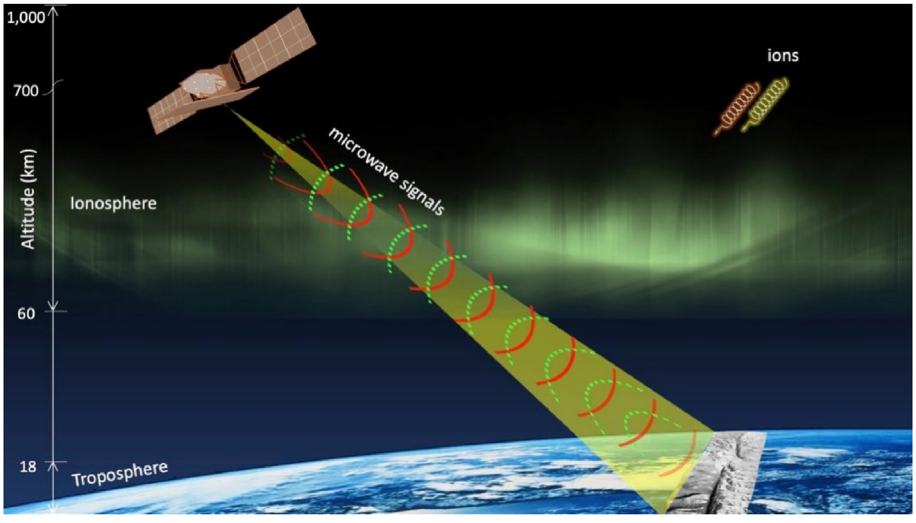

Fig. 1. A sketch of the observation geometry of the SAR system when traveling through the ionosphere.

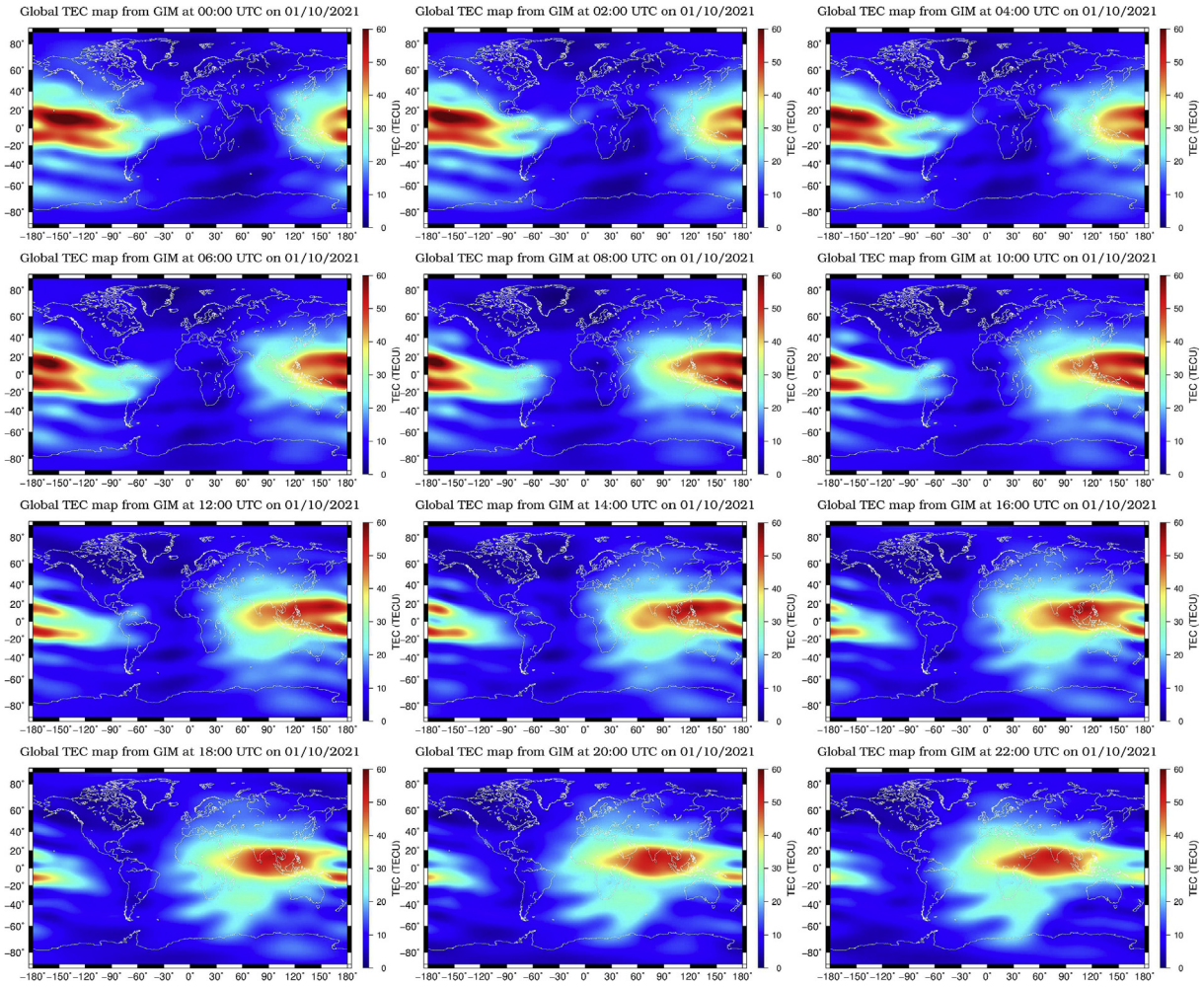

Fig. 2. Global Ionosphere Model (GIM) TEC maps from 00:00 to 22:00 on January 10, 2021. The data are from the International GNSS Service (IGS) global data center, European Space Agency.

ionospheric variations can be estimated using full-polarization SAR data. For the repeat-pass InSAR (single polarization), two kinds of measurements are usually contaminated by the ionosphere, i.e., the ionospheric artifacts on interferogram and pixel shifts on the azimuth offset map. Figs. 3 and 4 give examples of the effects of the ionosphere on single-pass full-polarization and repeat-pass InSAR data. The methods for mitigating the ionospheric propagation errors are presented in Section 3.

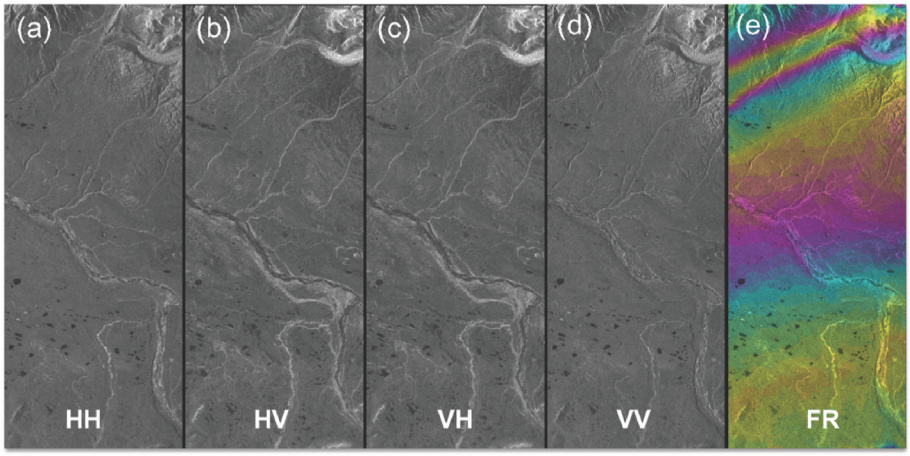

Fig. 3. An example of the ionospheric effect on full-polarization data. (a)–(d) SAR images from HH, HV, VH, and VV polarization, respectively. (e) FR angle due to the ionosphere.

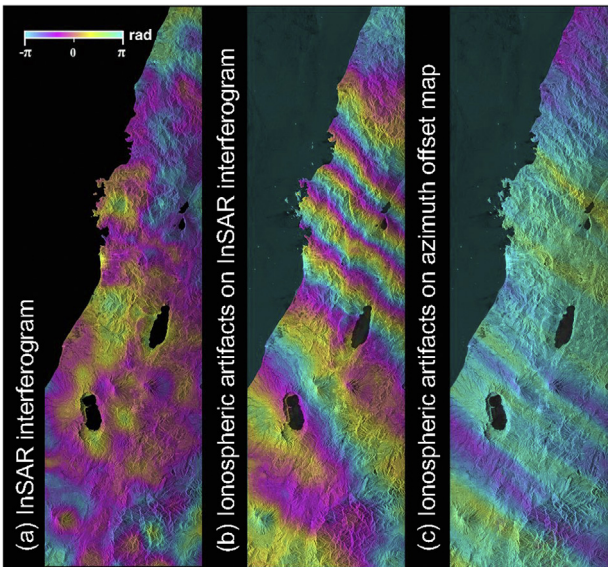

Fig. 4. An example of the ionospheric effect on InSAR data. (a) Interferogram without the ionospheric artifacts. (b) InSAR interferogram affected by the ionosphere. (c) Azimuth offset map affected by the ionosphere.

3. Methods for correcting ionospheric artifacts on InSAR

3.1. Faraday rotation method

When the SAR signal travels through the ionosphere, the polarization plane of the signal rotates to a certain degree depending on the magnitude of the electron density in the ionosphere, which is the so-called FR. Based on this magneto-ion property, the ionosphere-induced FR angle can be estimated from the full-polarization SAR data or dual-polarization data with prior information. The FR-based method is subsequently the earliest method used to study the ionosphere on SAR data [39]. Freeman [40] developed an effective way for correcting the ionospheric effects on full-polarization SAR data, where a step-by-step procedure was proposed to calibrate the full scattering matrix affected by the FR. Benefiting from the pioneer studies of Freeman, several studies have been consequently conducted to mitigate the ionosphere-induced FR for polarimetric SAR data, such as those from Advanced Land Observation Satellite (ALOS)/Phased Array L-band SAR (PALSAR) [41–44] and simulated BIOMASS (P-band) systems [45]. Due to the speckle noise on the SAR images, it is difficult to directly mitigate the ionospheric artifacts in InSAR using the FR-calibrated single SAR images. The degree of the FR angle is proportional to the vertical TEC (VTEC) map in the ionosphere. Kim [46] then proposed a method based on this relationship, and the results demonstrated the feasibility of the FR-based method in correcting the ionospheric contributions in the differential InSAR. However, the performance of the method is affected by some factors, such as the condition of the ionosphere, SNR of PolSAR data, number of looks in data processing, and geomagnetic latitude. Due to the geomagnetic field being almost perpendicular to the radar LOS direction, the FR-based method is not applicable around the equatorial latitudes [46]. The performance of the FR-based method was evaluated and compared with the azimuth shift method using the L-band PolSAR data in [47].

Fig. 5 shows an example of mitigating ionospheric artifacts over Thailand using the Faraday rotation method. Fig. 5(a) shows the original interferogram, mainly affected by the long-wavelength phase. The ionosphere-corrected interferogram based on the FR-derived ionospheric phase screen (IPS) is presented in Fig. 5(b). The long-wavelength phase contributions in Fig. 5(a) can be removed to a large extent, however, some long-wavelength signals still exist. Fig. 5(c) shows the interferogram with correction of the orbital phase using an orbital model. Most of the long-wavelength phase contributions cannot be removed if only the orbital phase model is used for correction. The interferogram corrected using the integrated phase model in [48] is shown in Fig. 5(d), and the long-wavelength phase contributions in Fig. 5(a) can be effectively removed. Comparison of Fig. 5(a) and (d) shows that in this case, the standard deviation of integration-corrected phase (0.46 rad) is reduced by approximately 28 times versus the original phase (12.83 rad). The residual phase in Fig. 5(d) is suspected to be contributed by the tropospheric and topographic phases.

3.2. Azimuth shift method

The azimuth shift-based method is originally from the discovery of the phenomenon of “azimuth streaks” in the interferometric pairs. Gray et al. [49] initially demonstrated the ionospheric effects in RADARSAT (C-band) and JERS-1 (L-band) data over the polar regions. Due to the fluctuations of the electron density in the ionosphere during SAR imaging, azimuth streaks are present as stripes with constant directions in the results of pixel offset or multi-aperture interferometry (MAI). Many studies have been devoted to exploring the potential for correcting the ionospheric effects based on this phenomenon [47,50–60].

A prototype method for mitigating the ionospheric artifacts based on this phenomenon is proposed by Matter and Gray [50]. Raucoules and de Michele [52] suggested a detailed procedure for mitigating the ionospheric artifacts, where the ionospheric azimuth shift is extracted using directional polynomial filtering from the result of azimuth pixel offset, and the scaling factor is estimated by the linear relation between the interferometric phase derivative and the ionospheric azimuth pixel shift. However, if the integral constant is not addressed, the IPS cannot be well estimated. Then, Jung et al. [54] developed a correction method based on the azimuth pixel offset from MAI. His method assumes that the deformation phase is not included in both the MAI and InSAR interferograms. To extend the applications to the areas with large-scale deformation, Zhang et al. [60] proposed a method to improve the estimation of the integral constant. In addition, a joint correction of ionospheric artifacts and orbital phase ramps was proposed in [56,58]. As verified with Global Positioning System (GPS) measurements, the accuracy can be improved approximately 60% with the azimuth shift-based method after correcting the ionospheric artifacts in the original InSAR interferogram [56,60].

Fig. 6 gives an example of the results of mitigating ionospheric artifacts of the 2008 M_w7.9 Wenchuan earthquake using the azimuth shift-based method in [60]. Fig. 6(a) and (c) show the azimuth and range pixel offset maps generated with MAI and offset tracking, respectively. The ionospheric azimuth pixel offset in Fig. 6(a) is in a constant direction and therefore can be separated from the deformation signals using directional filtering. Fig. 6(b) and (d) are the smoothed results of Fig. 6(a) and (c). Fig. 6(e) is the estimated IPS using the method in [60]. The original and ionospheric-corrected InSAR interferograms are shown in Fig. 6(f) and (g), respectively. The root-mean-squared (RMS) errors have decreased from 23.53 cm to 9.83 cm for Fig. 6(f) and (g) when comparing with GPS-observed LOS displacements, indicating the reliability of the azimuth shift method in ionospheric delay correction.

3.3. Range split-spectrum method

The range split-spectrum method is initially proposed to map the terrain elevations by calculating the absolute interferometric

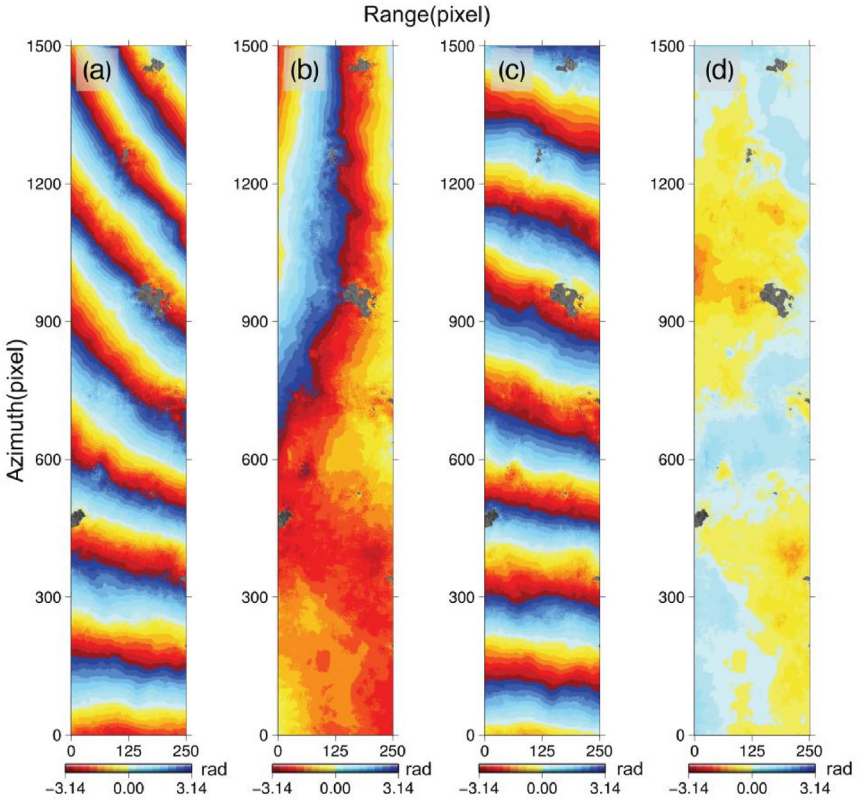

Fig. 5. Mitigation of the ionospheric artifacts by using the Faraday rotation method. (a) Original interferogram, (b) corrected interferogram by subtracting FR-derived ionospheric phase screen from (a), (c) interferogram with corrections of orbital phase from (a), and (d) interferogram by subtracting the FR-derived ionospheric phase screen and residual long-wavelength signals from (a). Reproduced from [48] with modifications.

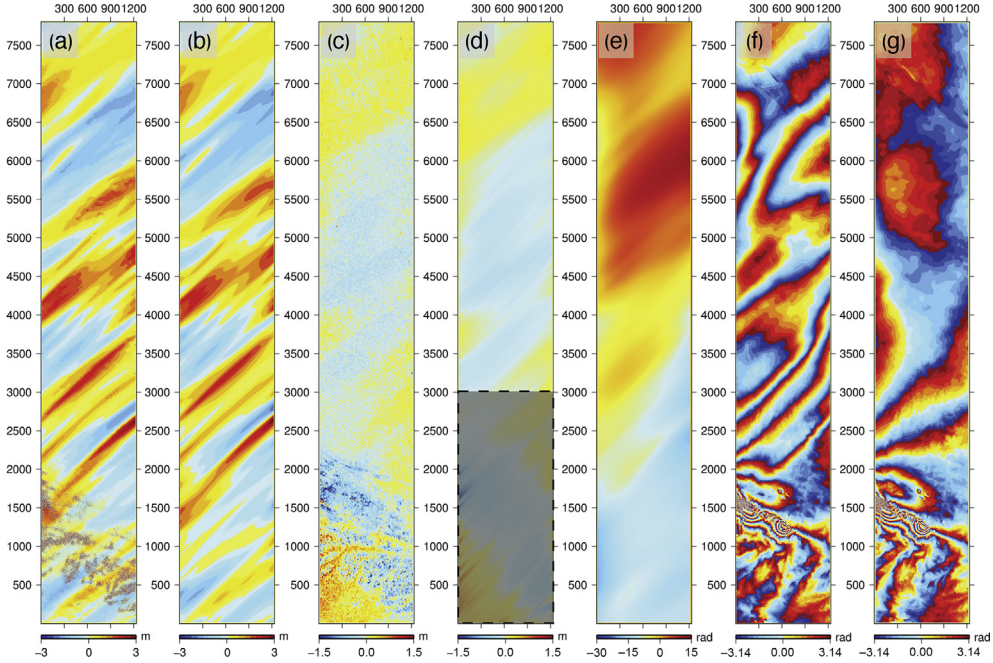

Fig. 6. Mitigation of the ionospheric artifacts in track 471 of the 2008 Wenchuan earthquake with ALOS PALSAR data. (a) Azimuth pixel offset map generated with MAI [61]. (b) Ionospheric azimuth pixel shift generated using adaptive directional filtering from (a). (c) Range pixel offset map produced by offset tracking [62]. (d) Smoothed range pixel offset map. (e) Estimated IPS. (f) Original InSAR interferogram. (g) Ionospheric-corrected InSAR interferogram. Reproduced from [60] with modifications.

phase [63,64]. It is implemented by separating the full range spectrum of SAR images into two sub-band spectrums with two different central frequencies, then the effective wavelength of the linearly synthetic interferogram will be significantly enlarged, and the absolute phase can be easily obtained by reducing the noise.

The basic idea of the range split-spectrum method is from the dispersive property of the ionosphere proposed in [65,66], where the signal traveling speed in the ionosphere is inversely proportional to the frequency of the microwave signal. Same as the dual-frequency GPS, if we simultaneously obtain two single look complex (SLC) images with two different central frequencies, the phase contributions in the InSAR interferogram can be separated into two components, i.e., non-dispersive and dispersive.

The dispersive component is contributed by the ionospheric phase term only, while the non-dispersive component consists of other phase terms, including deformation, topographic, orbital, and tropospheric. If the central frequency of sub-band SLC is equidistant from the central frequency of full-band SLC, the method can be called as symmetric range split-spectrum method, otherwise, it can be called as asymmetric range split-spectrum method. The latter one was proposed as the operational method for correcting the ionospheric artifacts of the data from the NISAR mission [67]. Then, the ionospheric phase component can be estimated from the interferograms generated by the sub-band SLC images.

However, two issues are also addressed in [66]. For example, the phase noise is greatly amplified due to the coefficient that is usually very large, and the unwrapped phase in the interferograms generated by the sub-band SLC images needs to be scaled before estimating the final IPS. Gomba et al. [68] proposed the practical implementation procedures for correcting the ionospheric artifacts based on this method. Although the basic principle of the method is very simple, if the procedures are not carefully carried out, the IPS can be poorly estimated and the correction cannot be effectively performed. These procedures include refinement of the interferogram, phase unwrapping correction of the sub-band interferograms, detection of the outliers, and smoothing of the IPS [68]. Recently, due to the effectiveness of the range split-spectrum technique, it has become the most popular method for estimating and removing the ionospheric phase contributions in InSAR. The method has extended to different observation modes and SAR missions, such as the terrain observation by progressive scans (TOPS) of Sentinel-1 and the scanning SAR (ScanSAR) of ALOS-2 [69,70]. Moreover, the method has been successfully applied to various applications and has enhanced the ability of InSAR to different scenarios, such as earthquake and glacier motion [71–75].

Fig. 7 shows an example of the results of mitigating the ionospheric artifacts of the M_W7.0 Kumamoto, Japan earthquake, which occurred on April 16, 2016. Fig. 7(a) is the original InSAR interferogram. Fig. 7(b) shows the azimuth pixel shift map presenting the ionospheric azimuth streaks. The ionospheric-corrected InSAR interferograms using symmetric and asymmetric range split-spectrum methods are displayed in Fig. 7(c)–(e). To quantitatively evaluate these results, we generated the normalized probability of the standard deviations from the symmetric and asymmetric methods (without smoothing). The standard deviation of symmetric and asymmetric range split-spectrum methods is highly consistent with the theoretical accuracy, as shown in Fig. 8. Even the standard deviations of the asymmetric range split-spectrum methods are worse than those of the optimal symmetric range split-spectrum method, but in the case of broadband SAR data, the deviation between these methods can be further improved by post-processing smoothing.

4. Discussion and recommendations

4.1. Current challenges

The methods for mitigating ionospheric phase contributions in the differential InSAR are applicable to different types of SAR data, the scale of variations in the ionosphere, and monitoring scenarios. For example, the FR-based method is only suitable to the full-polarization SAR data, and the rotation angle of the polarization plane cannot be directly estimated by the single- and dual-polarization data. However, full-polarization data for SAR missions are currently not frequently available and very limited in quantity. Moreover, the FR-based method is also limited due to the issues of parameter estimating, such as the inaccurate calibration parameters (i.e., crosstalk, channel imbalance, and additional noise) that introduce biases during the ionospheric correction, and imprecise parameters of the geomagnetic field that directly degrade the accuracy of the IPS estimation. The azimuth shift method is very sensitive to the small-scale variations in the ionosphere and has the potential to measure its variations at high resolution. However, there are three main issues with this method. First, the ionospheric azimuth shift is difficult to be isolated from the deformation when the direction of the azimuth streak is almost the same as the direction of azimuth deformation. Second, the final IPS will be biased if the parameters such as scaling, offset, and integral constant are not accurately estimated, especially when deformation signals cannot be well separated from the ionospheric phase. Third, this method is not applicable to the area with spatial gaps due to integration errors. Since the azimuth shift method only resolves the medium-scale ionospheric variations [37], the long-wavelength ionospheric component easily remains if the azimuth shift method is used alone, where the range split-spectrum method

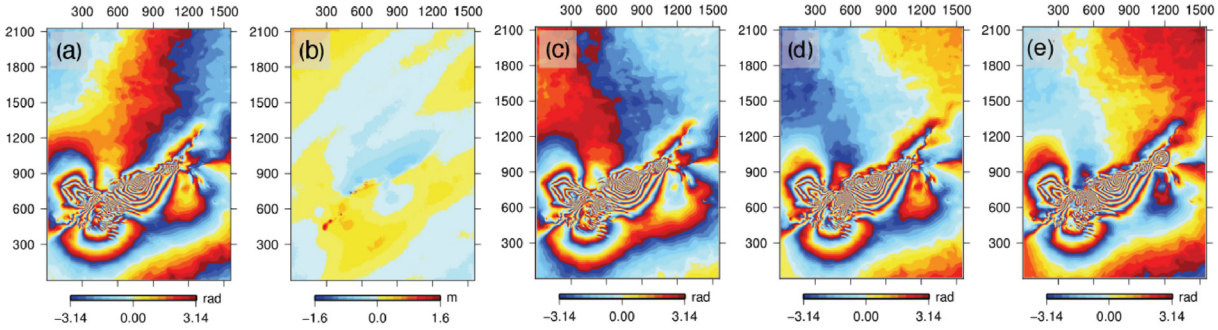

Fig. 7. Mitigation of the ionospheric artifacts of the 2016 Kumamoto earthquake using PALSAR-2 data. (a) Original InSAR interferogram. (b) Azimuth pixel shift map generated by MAI. Ionospheric-corrected InSAR interferogram using the (c) symmetric range split-spectrum method (one-third sub-bands), (d) asymmetric range split-spectrum method (one-fourth and one-sixteenth sub-bands), and (e) asymmetric range split-spectrum method (one-half and one-sixteenth sub-bands). Reproduced from [73] with modifications.

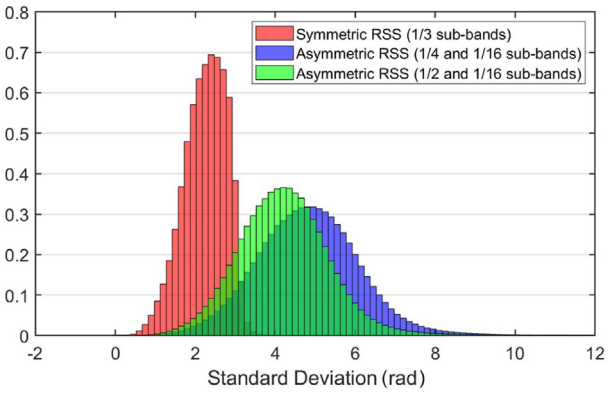

Fig. 8. Normalized probability of the standard deviation of the results from Fig. 7(c)–(e). Reproduced from [76] with modifications.

can be combined. The range split-spectrum method is effective for correcting the ionospheric artifacts in InSAR for the wideband SAR systems. However, this method is very sensitive to noise, and it can be largely amplified due to the split-spectrum processing and the linear combination of sub-band interferograms. For the interferometric pairs with low coherence, this method is challenging to be performed well [68].

The accuracy of the Faraday rotation method mainly depends on the center frequency of the SAR system, the effective look number, the polarimetric coherence, and the geomagnetic field along the integration path [77]. The value of the last factor decreases with increasing latitude, i.e., the accuracy of the Faraday rotation method generally increases from the equatorial regions to the polar regions. For the azimuth shift method, the accuracy is related to the central frequency of radar, the effective antenna length, the azimuth pixel spacing, the effective look number, the scaling factor, and the coherence of the MAI interferogram [54]. The accuracy of the range split spectrum method is mainly attributed to the central frequency and bandwidth of the SAR system, the effective look number, and the coherence of the sub-band interferogram [68]. Since the accuracy of these methods depends on different factors and may vary from case to case, how to adaptively combine the different methods for estimating the IPS is still challenging.

4.2. Recommendations for future research

Although some methods have been developed to mitigate the ionospheric artifacts, there are still some limitations for the individual-based method, as discussed in Section 4.1. Some studies have already demonstrated that a combination of methods from different groups can improve the estimation of the IPS, such as the combined use of the range split-spectrum method and azimuth shift method [37,78]. To improve the robustness of ionospheric corrections in InSAR, hybrid approaches based on each group of the methods are expected to be further integrated.

More and more SAR missions will be launched soon, with various imaging modes, such as the SweepSAR of NISAR [79] and the staggered stripmap of Tandem-L [80]. The ionospheric correction methods should be further adapted or developed for these new imaging modes, such as those presented for the TOPS mode of Sentinel-1 and the ScanSAR mode of ALOS-2 [69,70]. On the other hand, some algorithms improve the ability of InSAR applications but also change the methods of the traditional data processing, such as the Sequential Estimator [81] and the approach for "user-friendly" InSAR data [82]. Future work is needed to adapt the ionospheric correction for these new algorithms.

Among these methods, the azimuth shift method and range split-spectrum method can only estimate the differential ionospheric propagation errors, and the Faraday rotation method can measure the absolute ionospheric propagation errors [37,77]. If the azimuth shift or range split-spectrum method is applied for mitigating the ionospheric artifacts for multitemporal InSAR, the least square inversion can be applied to estimate the interval IPS from a connected network of IPS [83]. However, if the amount of the SAR image is very large, the computation will be very time-consuming. Developing methods for correcting the absolute ionospheric propagation errors in individual SLC images prior to the interferometric processing can highly reduce the computational time and improve the efficiency of the multitemporal InSAR.

5. Conclusions

InSAR has been broadly adopted to measure ground deformation, and it has experienced great success in the past three decades. However, when the SAR signals travel through the ionosphere, they may change in both space and time, and affect the measurement of InSAR. In this paper, we provide a review of the methods for mitigating the ionospheric artifacts in the differential InSAR and particularly focus on some of the most popular methods, such as the Faraday rotation, azimuth shift, and the range split spectrum methods. More effective and automatic methods are expected to be developed. By applying the ionospheric correction in InSAR, the understanding of the deformation induced by different activities will be less biased.

Conflicts of interest

The authors declare that there is no conflicts of interest.

Acknowledgments and Data

This work was supported by the National Key Research and Development Program of China (2020YFC1512001), the Guangdong Basic and Applied Basic Research Foundation (No. 2021A15 15011427), the Research Grants Council of the Hong Kong Special Administrative Region (Projects PolyU 152232/17E, PolyU 152164/18E and PolyU 152233/19E), the National Natural Science Foundation of China (Grants 41790445, 41974006, 42074040 and 41941019), the Shenzhen Scientific Research and Development Funding Program (Nos. 20200807110745001, KQJSCX20180328093453763 and 202008 12164904001), the Department of Education of Guangdong (218KTSCX196), the Fundamental Research Funds for the Central Universities (300102269207), the Research Institute for Sustainable Urban Development (RISUD) (BBWB), and the Innovation and Technology Fund of Hong Kong (ITP/019/20LP). The authors would like to thank the Japan Aerospace Exploration Agency (JAXA) for providing the ALOS PALSAR and ALOS-2 PALSAR-2 data under the RA6 PI Projects PI3380 and PI3232, and EO-RA2 Project ER2A2N040. Some of the ALOS PALSAR data were downloaded from the Alaska Satellite Facility (ASF) Distributed Active Archive Center (DAAC) website (https://vertex.daac.asf.alaska.edu/) and are copyrighted to JAXA/METI. Some of the figures were generated by Generic Mapping Tools (GMT 5.2.1) software (http://gmt.soest.hawaii.edu).

References

[1] H.A. Zebker, R.M. Goldstein, Topographic mapping from interferometric synthetic aperture radar observations, J. Geophys. Res. Solid Earth 91 (B5) (1986) 4993–4999, https://doi.org/10.1029/JB091iB05p04993.
[2] D. Massonnet, K.L. Feigl, Radar interferometry and its application to changes in the earth's surface, Rev. Geophys. 36 (4) (1998) 441–500, https://doi.org/10.1029/97RG03139.

[3] X. Qin, et al., A structure knowledge-synthetic aperture radar interferometry integration method for high-precision deformation monitoring and risk identification of sea-crossing bridges, Int. J. Appl. Earth Obs. 103 (2021) 102476, https://doi.org/10.1016/j.jag.2021.102476.
[4] D. Massonnet, et al., The displacement field of the landers earthquake mapped by radar interferometry, Nature 364 (6433) (1993) 138–142, https://doi.org/10.1038/364138a0.
[5] Z.K. Shen, et al., Slip maxima at fault junctions and rupturing of barriers during the 2008 Wenchuan earthquake, Nat. Geosci. 2 (10) (2009) 718–724, https://doi.org/10.1038/ngeo636.
[6] R.M. Goldstein, H. Engelhardt, B. Kamb, R.M. Frolich, Satellite radar interferometry for monitoring ice sheet motion: application to an antarctic ice stream, Science 262 (5139) (Dec 3 1993) 1525–1530, https://doi.org/10.1126/science.262.5139.1525.
[7] E. Rignot, et al., Recent Antarctic ice mass loss from radar interferometry and regional climate modelling, Nat. Geosci. 1 (2) (2008) 106–110, https://doi.org/10.1038/ngeo102.
[8] F. Amelung, S. Jónsson, H. Zebker, P. Segall, Widespread uplift and 'trapdoor' faulting on Galapagos volcanoes observed with radar interferometry, Nature 407 (6807) (2000) 993, https://doi.org/10.1038/35039604.
[9] J. Biggs, et al., Global link between deformation and volcanic eruption quantified by satellite imagery, Nat. Commun. 5 (1) (2014) 1–7, https://doi.org/10.1038/ncomms4471.
[10] C. Carnec, C. Delacourt, Three years of mining subsidence monitored by SAR interferometry, near Gardanne, France, J. Appl. Geophys. 43 (1) (2000) 43–54, https://doi.org/10.1016/S0926-9851(99)00032-4.
[11] J.W. Bell, F. Amelung, A. Ferretti, M. Bianchi, F. Novali, Permanent scatterer InSAR reveals seasonal and long-term aquifer-system response to groundwater pumping and artificial recharge, Water Resour. Res. 44 (2) (2008), https://doi.org/10.1029/2007WR006152.
[12] X. Ding, G. Liu, Z. Li, Z. Li, Y. Chen, Ground subsidence monitoring in Hong Kong with satellite SAR interferometry, Photogramm. Eng. Remote Sens. 70 (10) (2004) 1151–1156, https://doi.org/10.14358/PERS.70.10.1151.
[13] S. Wu, X. Ding, B. Zhang, Continuous monitoring the ground deformation by a step-by-step estimator in MTInSAR, in: IGARSS 2019-2019 IEEE Int. Geosci. Remote Sens. Symp., IEEE, 2019, pp. 1994–1997, https://doi.org/10.1109/IGARSS.2019.8898400.
[14] S. Wu, B. Zhang, H. Liang, C. Wang, X. Ding, L. Zhang, Detecting the deformation anomalies induced by underground construction using multiplatform MT-InSAR: a case study in to Kwa wan Station, Hong Kong, IEEE J. Sel. Top. Appl. Earth Obs. 14 (2021) 9803–9814, https://doi.org/10.1109/JSTARS.2021.3113672.
[15] S. Xiong, C. Wang, X. Qin, B. Zhang, Q. Li, Time-series analysis on persistent scatter-interferometric synthetic aperture radar (PS-InSAR) derived displacements of the Hong Kong–Zhuhai–Macao Bridge (HZMB) from Sentinel-1A observations, Remote Sens. 13 (4) (2021) 546, https://doi.org/10.3390/rs13040546.
[16] X. Qin, L. Zhang, M. Yang, H. Luo, M. Liao, X. Ding, Mapping surface deformation and thermal dilation of arch bridges by structure-driven multi-temporal DInSAR analysis, Remote Sens. Environ. 216 (2018) 71–90, https://doi.org/10.1016/j.rse.2018.06.032.
[17] X. Ding, Z. Li, J. Zhu, G. Feng, J. Long, Atmospheric effects on InSAR measurements and their mitigation, Sensors 8 (9) (2008) 5426–5448, https://doi.org/10.3390/s8095426.
[18] Z. Li, et al., Time-series InSAR ground deformation monitoring: atmospheric delay modeling and estimating, Earth Sci. Rev. (2019), https://doi.org/10.1016/j.earscirev.2019.03.008.
[19] F. Meyer, R. Bamler, N. Jakowski, T. Fritz, The potential of low-frequency SAR systems for mapping ionospheric TEC distributions, IEEE Geosci. Remote Sens.Lett. 3 (4) (2006) 560–564, https://doi.org/10.1109/LGRS.2006.882148.
[20] D. Bekaert, R. Walters, T. Wright, A. Hooper, D. Parker, Statistical comparison of InSAR tropospheric correction techniques, Remote Sens. Environ. 170 (2015) 40–47, https://doi.org/10.1016/j.rse.2015.08.035.
[21] S. Pulinets, Seismic activity as a source of the ionospheric variability, Adv. Space Res. 22 (6) (1998) 903–906, https://doi.org/10.1016/S0273-1177(98)00121-5.
[22] K. Davies, Ionospheric Radio (No. 31), Institution of Engineering and Technology, London, United Kingdom, 1990.
[23] Z.-W. Xu, J. Wu, Z.-S. Wu, A survey of ionospheric effects on space-based radar, Waves Random Media 14 (2004) S189–S273, https://doi.org/10.1109/TGRS.2015.2468573.
[24] F.J. Meyer, K. Chotoo, S.D. Chotoo, B.D. Huxtable, C.S. Carrano, The influence of equatorial scintillation on L-band SAR image quality and phase, IEEE Trans. Geosci. Remote Sens. 54 (2) (2016) 869–880, https://doi.org/10.1109/TGRS.2015.2468573.
[25] R. Bamler, P. Hartl, Synthetic aperture radar interferometry, Inverse Probl. 14 (1998) R1–R54, https://doi.org/10.1088/0266-5611/14/4/001.
[26] M. Simons, P. Rosen, Interferometric synthetic aperture radar geodesy, in: G. Schubert (Ed.), Treatise on Geophysics, vol. 3, Elsevier Press, 2007, pp. 391–446, https://doi.org/10.1016/B978-044452748-6.00059-6.
[27] H. Liang, L. Zhang, Z. Lu, X. Li, Nonparametric estimation of DEM error in multitemporal InSAR, IEEE Trans. Geosci. Remote Sens. 57 (12) (2019) 10004–10014, https://doi.org/10.1109/TGRS.2019.2930802.
[28] P. Agram, M. Simons, A noise model for InSAR time series, J. Geophys. Res. Solid Earth 120 (4) (2015) 2752–2771, https://doi.org/10.1002/2014JB011271.
[29] L. Zhang, X. Ding, Z. Lu, H.-S. Jung, J. Hu, G. Feng, A novel multitemporal InSAR model for joint estimation of deformation rates and orbital errors, IEEE Trans. Geosci. Remote Sens. 52 (6) (2013) 3529–3540, https://doi.org/10.1109/TGRS.2013.2273374.
[30] H. Fattahi, F. Amelung, InSAR uncertainty due to orbital errors, Geophys. J. Int. 199 (1) (2014) 549–560, https://doi.org/10.1093/gji/ggu276.
[31] Y. Du, H. Fu, L. Liu, G. Feng, X. Peng, D. Wen, Orbit error removal in InSAR/MTInSAR with a patch-based polynomial model, Int. J. Appl. Earth Obs. Geoinf. 102 (2021) 102438, https://doi.org/10.1016/j.jag.2021.102438.
[32] A. Ferretti, A. Fumagalli, F. Novali, C. Prati, F. Rocca, A. Rucci, A new algorithm for processing interferometric data-stacks: SqueeSAR, IEEE Trans. Geosci. Remote Sens. 49 (9) (2011) 3460–3470, https://doi.org/10.1109/TGRS.2011.2124465.
[33] M. Jiang, Sentinel-1 TOPS co-registration over low-coherence areas and its application to velocity estimation using the all pairs shortest path algorithm, J. Geod. 94 (10) (2020) 1–15, https://doi.org/10.1007/s00190-020-01432-1.
[34] M. Jiang, A.M. Guarnieri, Distributed scatterer interferometry with the refinement of spatiotemporal coherence, IEEE Trans. Geosci. Remote Sens. 58 (6) (2020) 3977–3987, https://doi.org/10.1109/TGRS.2019.2960007.
[35] R. Bürgmann, P.A. Rosen, E.J. Fielding, Synthetic aperture radar interferometry to measure earth's surface topography and its deformation, Annu. Rev. Earth Planet. Sci. 28 (1) (2000) 169–209, https://doi.org/10.1146/annurev.earth.28.1.169.
[36] P. Rosen, et al., Synthetic aperture radar interferometry, Proc. IEEE 88 (3) (2000) 333–382, https://doi.org/10.1109/5.838084.
[37] G. Gomba, F. De Zan, Bayesian data combination for the estimation of ionospheric effects in SAR interferograms, IEEE Trans. Geosci. Remote Sens. 55 (11) (2017) 6582–6593, https://doi.org/10.1109/TGRS.2017.2730438.
[38] F. Meyer, A review of ionospheric effects in low-frequency SAR—signals, correction methods, and performance requirements, in: IGARSS 2010-2010 IEEE Int. Geosci. Remote Sens. Symp., IEEE, 2010, pp. 29–32, https://doi.org/10.1109/IGARSS.2010.5654258.
[39] S. Bickel, R. Bates, Effects of magneto-ionic propagation on the polarization scattering matrix, Proc. IEEE 53 (8) (1965) 1089–1091, https://doi.org/10.1109/PROC.1965.4097.
[40] A. Freeman, Calibration of linearly polarized polarimetric SAR data subject to Faraday rotation, IEEE Trans. Geosci. Remote Sens. 42 (8) (2004) 1617–1624, https://doi.org/10.1109/TGRS.2004.830161.
[41] G. Sandberg, L.E. Eriksson, L.M. Ulander, Measurements of Faraday rotation using polarimetric PALSAR images, IEEE Geosci. Remote Sens.Lett. 6 (1) (2008) 142–146, https://doi.org/10.1109/LGRS.2008.2010062.
[42] H. Kimura, Calibration of polarimetric PALSAR imagery affected by Faraday rotation using polarization orientation, IEEE Trans. Geosci. Remote Sens. 47 (12) (2009) 3943–3950, https://doi.org/10.1109/TGRS.2009.2028692.
[43] A. Takeshiro, T. Furuya, H. Fukuchi, Verification of polarimetric calibration method including Faraday rotation compensation using PALSAR data, IEEE Trans. Geosci. Remote Sens. 47 (12) (2009) 3960–3968, https://doi.org/10.1109/TGRS.2009.2034465.
[44] N.C. Rogers, S. Quegan, The accuracy of Faraday rotation estimation in satellite synthetic aperture radar images, IEEE Trans. Geosci. Remote Sens. 52 (8) (2013) 4799–4807, https://doi.org/10.1109/TGRS.2013.2284635.
[45] J.S. Kim, K.P. Papathanassiou, S. Quegan, N. Rogers, Estimation and correction of scintillation effects on spaceborne P-band SAR images, in: 2012 IEEE Int. Geosci.Remote Sens. Symp., IEEE, 2012, pp. 5101–5104, https://doi.org/10.1109/IGARSS.2012.6352463.
[46] J.S. Kim, Development of Ionosphere Estimation Techniques for the Correction of SAR Data, ETH Zurich, 2013, https://doi.org/10.3929/ethz-a-010077304.
[47] W. Zhu, X.-L. Ding, H.-S. Jung, Q. Zhang, Mitigation of ionospheric phase delay error for SAR interferometry: an application of FR-based and azimuth offset methods, Remote Sens. Lett. 8 (1) (2017) 58–67, https://doi.org/10.1080/2150704X.2016.1235808.
[48] W. Zhu, H.-S. Jung, J.-Y. Chen, Synthetic aperture radar interferometry (InSAR) ionospheric correction based on Faraday rotation: two case studies, Appl. Sci. 9 (18) (2019) 3871, https://doi.org/10.3390/app9183871.
[49] A.L. Gray, K.E. Mattar, G. Sofko, Influence of ionospheric electron density fluctuations on satellite radar interferometry, Geophys. Res. Lett. 27 (10) (2000) 1451–1454, https://doi.org/10.1029/2000GL000016.
[50] K. Mattar, A. Gray, Reducing ionospheric electron density errors in satellite radar interferometry applications, Can. J. Remote Sens. 28 (4) (2002) 593–600, https://doi.org/10.5589/m02-051.
[51] U. Wegmuller, C. Werner, T. Strozzi, A. Wiesmann, Ionospheric electron concentration effects on SAR and INSAR, in: IGARSS 2006, IEEE, Denver, USA, 2006, pp. 3731–3734, https://doi.org/10.1109/IGARSS.2006.956.
[52] D. Raucoules, M. De Michele, Assessing ionospheric influence on L-band SAR data: implications on coseismic displacement measurements of the 2008 Sichuan earthquake, IEEE Geosci. Remote Sens.Lett. 7 (2) (2010) 286–290, https://doi.org/10.1109/LGRS.2009.2033317.
[53] J. Hu, et al., Correcting ionospheric effects and monitoring two-dimensional displacement fields with multiple-aperture InSAR technology with application to the Yushu earthquake, Sci. China Earth Sci. 55 (12) (2012) 1961–1971, https://doi.org/10.1007/s11430-012-4509-x.

[54] H.S. Jung, D.T. Lee, Z. Lu, J.S. Won, Ionospheric correction of SAR interferograms by multiple-aperture interferometry, IEEE Trans. Geosci. Remote Sens. 51 (5) (2012) 3191–3199, https://doi.org/10.1109/TGRS.2012.2218660.
[55] U. Wegmuller, T. Strozzi, C. Werner, Ionospheric path delay estimation using split-beam interferometry, in: Proc. Int. Geosci. Remote Sens. Symp. (IGARSS'12), 2012 IEEE International, IEEE, 2012, pp. 3631–3634, https://doi.org/10.1109/IGARSS.2012.6350630.
[56] Z. Liu, H.-S. Jung, Z. Lu, Joint correction of ionosphere noise and orbital error in L-band SAR interferometry of interseismic deformation in southern California, IEEE Trans. Geosci. Remote Sens. 52 (6) (2013) 3421–3427, https://doi.org/10.1109/TGRS.2013.2272791.
[57] A.C. Chen, H.A. Zebker, Reducing ionospheric effects in InSAR data using accurate coregistration, IEEE Trans. Geosci. Remote Sens. 52 (1) (2014) 60–70, https://doi.org/10.1109/TGRS.2012.2236098.
[58] H.-S. Jung, W.-J. Lee, An improvement of ionospheric phase correction by multiple-aperture interferometry, IEEE Trans. Geosci. Remote Sens. 53 (9) (2015) 4952–4960, https://doi.org/10.1109/TGRS.2015.2413948.
[59] G. Gomba, F. De Zan, A. Parizzi, Compensation of Ionospheric Azimuth Shifts Using Azimuth Sub-apertures Interferometry, 2016.
[60] B. Zhang, X. Ding, W. Zhu, C. Wang, L. Zhang, Z. Liu, Mitigating ionospheric artifacts in coseismic interferogram based on offset field derived from ALOS-PALSAR data, IEEE J. Sel. Top. Appl. Earth Obs. Remote Sens. 9 (7) (2016) 3050–3059, https://doi.org/10.1109/JSTARS.2016.2533441.
[61] N.B.D. Bechor, H.A. Zebker, Measuring two-dimensional movements using a single InSAR pair, Geophys. Res. Lett. 33 (16) (2006) L16311, https://doi.org/10.1029/2006GL026883.
[62] T. Strozzi, A. Luckman, T. Murray, U. Wegmuller, C.L. Werner, Glacier motion estimation using SAR offset-tracking procedures, IEEE Trans. Geosci. Remote Sens. 40 (11) (2002) 2384–2391, https://doi.org/10.1109/TGRS.2002.805079.
[63] S.N. Madsen, H.A. Zebker, Automated absolute phase retrieval in across-track interferometry, in: IGARSS 1992, IEEE, Houston, 1992, pp. 1582–1584, https://doi.org/10.1109/IGARSS.1992.578639.
[64] S.N. Madsen, Absolute phase determination techniques in SAR interferometry, in: Algorithms for Synthetic Aperture Radar Imagery II, vol. 2487, International Society for Optics and Photonics, 1995, pp. 393–402, https://doi.org/10.1117/12.210860. https://ui.adsabs.harvard.edu/link_gateway/1995SPIE.2487.393M/.
[65] R. Brcic, A. Parizzi, M. Eineder, R. Bamler, F. Meyer, Estimation and compensation of ionospheric delay for SAR interferometry, in: 2010 IEEE Int. Geosci. Remote Sens. Symp. (IGARSS), IEEE, 2010, pp. 2908–2911, https://doi.org/10.1109/IGARSS.2010.5652231.
[66] P. Rosen, S. Hensley, C. Chen, Measurement and mitigation of the ionosphere in L-band Interferometric SAR data, in: Radar Conference 2010, IEEE, Washington DC, 2010, pp. 1459–1463, https://doi.org/10.1109/RADAR.2010.5494385.
[67] P. Rosen, et al., An update on the NASA-ISRO dual-frequency DBF SAR (NISAR) mission, in: 2016 IEEE Int. Geosci. Remote Sens. Symp. (IGARSS), IEEE, 2016, pp. 2106–2108, https://doi.org/10.1109/IGARSS.2016.7729543.
[68] G. Gomba, A. Parizzi, F. De Zan, M. Eineder, R. Bamler, Toward operational compensation of ionospheric effects in SAR interferograms: the split-spectrum method, IEEE Trans. Geosci. Remote Sens. 54 (3) (2016) 1446–1461, https://doi.org/10.1109/TGRS.2015.2481079.
[69] G. Gomba, F.R. González, F. De Zan, Ionospheric phase screen compensation for the Sentinel-1 TOPS and ALOS-2 ScanSAR modes, IEEE Trans. Geosci. Remote Sens. 55 (1) (2017) 223–235, https://doi.org/10.1109/TGRS.2016.2604461.
[70] C. Liang, E.J. Fielding, Interferometry with ALOS-2 full-aperture ScanSAR data, IEEE Trans. Geosci. Remote Sens. 55 (5) (2017) 2739–2750, https://doi.org/10.1109/TGRS.2017.2653190.
[71] I.J. Hamling, et al., Complex multifault rupture during the 2016 M w 7.8 Kaikōura earthquake, New Zealand, Science 356 (6334) (2017) eaam7194, https://doi.org/10.1126/science.aam7194.
[72] H. Liao, F.J. Meyer, B. Scheuchl, J. Mouginot, I. Joughin, E. Rignot, Ionospheric correction of InSAR data for accurate ice velocity measurement at polar regions, Remote Sens. Environ. 209 (2018) 166–180, https://doi.org/10.1016/j.rse.2018.02.048.
[73] B. Zhang, X. Ding, W. Zhu, An asymmetric split-spectrum method for estimating the ionospheric artifacts in insar data, in: 2018 IEEE Int. Geosci. Remote Sens. Symp. (IGARSS), IEEE, 2018, pp. 517–520, https://doi.org/10.1109/IGARSS.2018.8518936.
[74] B. Zhang, C. Wang, X. Ding, W. Zhu, S. Wu, Correction of ionospheric artifacts in SAR data: application to fault slip inversion of 2009 southern Sumatra earthquake, IEEE Geosci. Remote Sens.Lett. 15 (9) (2018) 1327–1331, https://doi.org/10.1109/LGRS.2018.2844686.
[75] B. Zhang, et al., Impact of ionosphere on InSAR observation and coseismic slip inversion: improved slip model for the 2010 Maule, Chile, earthquake, Remote Sens. Environ. 267 (2021) 112733, https://doi.org/10.1016/j.rse.2021.112733.
[76] B. Zhang, Mitigation of Ionospheric Artifacts in InSAR Data for Estimating Earthquake Deformation, Ph.D., Department of Land Surveying and Geo-Informatics, Hong Kong Polytechnic University, Hong Kong, 2020 https://theses.lib.polyu.edu.hk/handle/200/10486.
[77] J.S. Kim, K.P. Papathanassiou, R. Scheiber, S. Quegan, Correcting distortion of polarimetric SAR data induced by ionospheric scintillation, IEEE Trans. Geosci. Remote Sens. 53 (12) (2015) 6319–6335, https://doi.org/10.1109/TGRS.2015.2431856.
[78] W. Mao, et al., An InSAR ionospheric correction method based on variance component estimation with integration of MAI and RSS measurements, IEEE J. Sel. Top. Appl. Earth Obs. Remote Sens. 14 (2020) 1423–1433, https://doi.org/10.1109/JSTARS.2020.3045267.
[79] A. Freeman, et al., DESDynI–A NASA mission for ecosystems, solid Earth, and cryosphere science, in: PolInSAR 2009, Frascati, Italy, 2009, pp. 26–30.
[80] M. Villano, G. Krieger, A. Moreira, Staggered SAR: high-resolution wide-swath imaging by continuous PRI variation, IEEE Trans. Geosci. Remote Sens. 52 (7) (2014) 4462–4479, https://doi.org/10.1109/TGRS.2013.2282192.
[81] H. Ansari, F. De Zan, R. Bamler, Sequential estimator: toward efficient InSAR time series analysis, IEEE Trans. Geosci. Remote Sens. 55 (10) (2017) 5637–5652, https://doi.org/10.1109/TGRS.2017.2711037.
[82] H.A. Zebker, User-friendly InSAR data products: fast and simple timeseries processing, IEEE Geosci. Remote Sens.Lett. 14 (11) (2017) 2122–2126, https://doi.org/10.1109/LGRS.2017.2753580.
[83] H. Fattahi, M. Simons, P. Agram, InSAR time-series estimation of the ionospheric phase delay: an extension of the split range-spectrum technique, IEEE Trans. Geosci. Remote Sens. 55 (10) (2017) 5984–5996, https://doi.org/10.1109/TGRS.2017.2718566.

Bochen Zhang received the B.Eng. degree in geodesy and geomatics from the Nanjing University of Technology, Nanjing, China, in 2010, the M.Sc. degree in geomatics, and the Ph.D. degree in geodesy and geodynamics from The Hong Kong Polytechnic University, Hong Kong, in 2012 and 2020, respectively. He is currently an Assistant Professor with the College of Civil and Transportation Engineering, Shenzhen University, Shenzhen, China. His research interests include developing techniques for spaceborne and terrestrial radar interferometric data processing, with emphasis on geohazards and infrastructures monitoring.

Wu Zhu received the M.Sc. degree in geodesy and geodynamics from Chang'an University, Xi'an, China, in 2010 and Ph.D. degree in the Department of Land Surveying and Geo-Informatics (LSGI), The Hong Kong Polytechnic University, Kowloon, Hong Kong, in 2015. His research interests include estimation and correction of ionospheric effects on interferometric synthetic aperture radar (InSAR), analyses of InSAR-measured surface deformation associated with the geophysical hazards.

Xiaoli Ding received B.Eng. from Central South University of Metallurgy, Changsha, China, in 1983 and Ph.D. from the University of Sydney, Australia, in 1993. He is currently Chair Professor of Geomatics in Department of Land Surveying and Geo-Informatics, The Hong Kong Polytechnic University, Hong Kong. He lectured at the Northeast University of Technology, Shenyang, China (in 1983–1986), and Curtin University of Technology, Perth, Australia (in 1992–1996), before joining The Hong Kong Polytechnic University in 1996. His main research interests are in developing technologies for studying ground and structural deformation and geohazards.

Chisheng Wang received the B.S. degree from Beijing Normal University, Beijing, China, in 2007, the M.S. degree from the Institute of Applied Remote Sensing, Chinese Academy of Science, Beijing, in 2010, and the Ph.D. degree from the Department of Land Surveying and Geo-Informatics, The Hong Kong Polytechnic University, Kowloon, Hong Kong. He is currently an Assistant Professor with the Guangdong Key Laboratory of Urban Informatics, School of Architecture & Urban Planning, Shenzhen University, Shenzhen, Guangdong, China. His research interests include image processing and remote sensing applications.

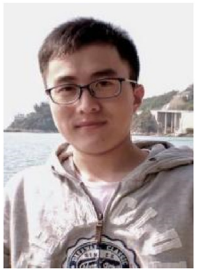

Songbo Wu received the B.S. degree from Xinjiang University, Xinjiang, China, in 2012, the M.Sc. degree from South-West Jiaotong University, Sichuan, China, in 2015. He is currently working toward the Ph.D. degree in geodesy and geodynamics from the Department of Land Surveying and Geo-Informatics (LSGI), The Hong Kong Polytechnic University, Kowloon, Hong Kong. His research interests include SAR image processing for multitemporal synthetic aperture radar interferometry and the applications on ground deformation continuous monitoring.

Qin Zhang received the M.S. and Ph.D. degrees in geodesy and geodynamics from Wuhan University, Wuhan, China, in 1994 and 2002, respectively. She is currently the professor with the school of Geology Engineering and Geomatics, Chang'an University, Xi'an, China. Her research interest focus on the GNSS, InSAR, surveying adjustment, crustal deformation and geological hazard monitoring. Prof.Zhang has hold a large number of research projects funded by universities and governments, and she published more than 200 technic papers in different journals.